OUT-OF-PLANE CYCLIC TESTING OF TALL REINFORCED MASONRY WALLS

F. Mosele[1], F. da Porto[2] and C. Modena[3]

[1]*PhD Candidate,* [2]*Assistant Professor,* [3]*Full Professor, Dept. of Structural and Transportation Engineering , University of Padua, Padua, Italy*
Email: mosele@dic.unipd.it, daporto@dic.unipd.it, modena@dic.unipd.it

ABSTRACT :

In the framework of the DISWall research project, funded by the European Commission, innovative construction systems, based on the use of perforated clay units and aimed at building mainly tall, load bearing reinforced masonry walls for one-storey industrial and commercial buildings, were developed. In these cases, very often buildings are provided with deformable roofs, made with prefabricated elements or glulam beams. In the case of seismic actions, deformable roofs are not able to redistribute horizontal actions to in-plane walls. Walls orthogonal to seismic load direction can be tentatively considered as cantilevers, with vertical load applied at the top and horizontal out of plane load, due to the seismic action associated to the masses of both roof and wall itself. For this structural configuration, two real scale frames, composed by two parallel reinforced masonry walls, 6 m in height, vertically loaded by steel/concrete slab, were built and subjected to cyclic tests, by applying horizontal loads at the top slab level. The aim was studying tall walls' behaviour under out-of-plane loads and P-Δ effects. In the present contribution, results of experimental tests and analysis of bending moments are presented.

KEYWORDS: reinforced masonry, cyclic tests, out-of-plane tests, one-storey tall buildings, industrial buildings.

1. INTRODUCTION

In the last decades, a large variety of reinforced masonry techniques have been made available, with different geometric shape and material of units, composition of mortar and/or grout, quantity and layout of reinforcement (Tomaževič 1999). Developments are generally aimed at improving the in-plane behavior of walls, as the basic principles of conceptual design of structures for earthquake resistance are based on the box-type of behavior. With this assumption, horizontal seismic actions are transferred to walls parallel to the direction of load application (Shing et al. 1990).
In the case of single-story tall buildings, such as commercial and industrial buildings, the use of slender load-bearing walls can be useful, as they are technological solution with several advantages regarding not only the structural, but also the environmental requirements. In these cases, reinforced load-bearing masonry walls, compared to other systems including framed structures, assure that controlled thermo-hygrometric conditions are respected, without the use of insulating or coating materials. At the same time, it has been recognized that the effect of transverse loads, such as wind loading, earth pressure, and inertia forces from seismic excitation, are significant for slender walls (Bean Popehn et al. 2007).
Static and dynamic tests of unreinforced, post-tensioned and strengthened slender masonry walls, under out-of-plane loading and with pin supports at both ends, have been carried out also recently (see, for example, Bean Popehn et al. 2007 and Griffith et al. 2004). This corresponds to situations where the structure has 'stiff' horizontal floor diaphragm and walls are well connected to floors. Less frequently, experimental tests, accounting also for possible presence of deformable roofs, were carried out to evaluate dynamic out-of-plane response of unreinforced and strengthened masonry

walls (Ewing and Kariotis 1981; Simsir et al. 2003). In the case of the current research, interest was focused on this type of aspects. In fact, roofs for sport and commercial centers, as well as those for industrial buildings, very often are, for aesthetical or economical reasons, built with deformable structures. The main aim of the experimental research carried out was thus studying, with quasi-static cyclic procedures, out-of-plane behavior of two reinforced masonry systems, used for the construction of tall walls (6-8m high) in single-story commercial and industrial buildings.

2. EXPERIMENTAL PROGRAM

2.1. Reinforced Masonry Systems

The studied reinforced masonry systems are based on the use of vertically perforated clay units, with concentrated reinforcement. The first system (Figure 1a) employs 'H' shaped units, where limited quantity of vertical reinforcement, aligned on the middle plane of wall, can be inserted. The second system, developed starting from the first (Figure 1b) is based on the use of 'C' shaped units, alternate with 'H' ones. 'C' units have large central core (140x110 mm), which allows placing higher quantity of reinforcement and un-coupling the reinforcement bars. Furthermore, 'C' units can be laid around the vertical reinforcement. The construction process is thus simplified, as 'H' units, on the contrary, need to be threaded on to the reinforcement bars. Finally, with 'C' shaped units, overlapping of reinforcement can be avoided, allowing more effective inter-storey high rebars to be used.

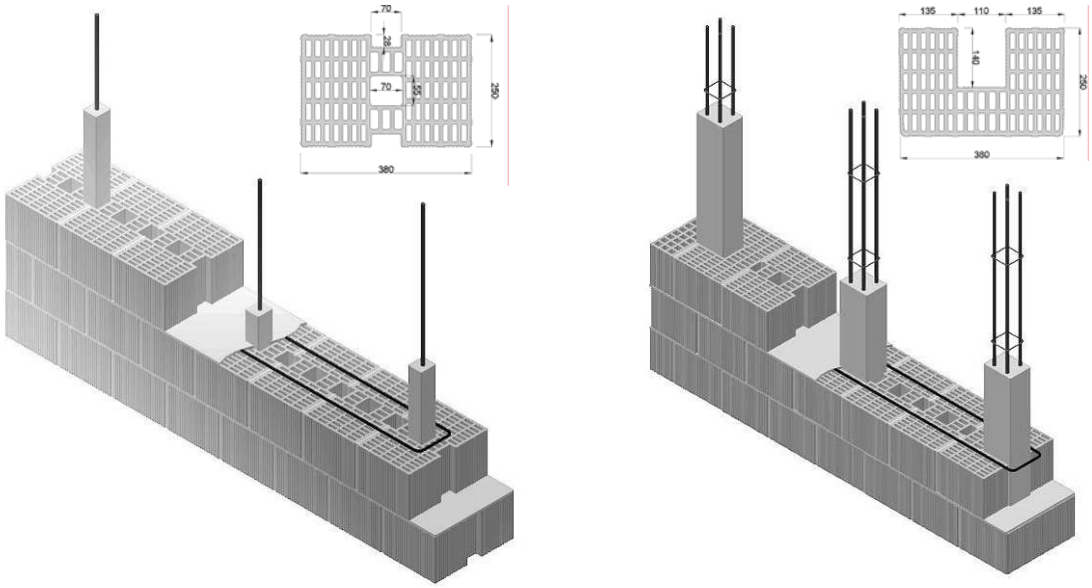

(a) rmH (b) rmC

Figure 1 Construction systems

The two used units had same overall dimensions (250x380x190 mm respectively for length, width and height, Figure 1), and percentage of holes less than 45%. They showed similar behavior in compression, with average compressive strength of about 12 N/mm^2 and average elastic modulus of 11.6 kN/mm^2. Vertical reinforcement was constituted, for the 'H' shaped unit reinforced masonry system, by 1 ribbed rebar with diameter of 16 mm (Figure 1a); while it was constituted, for the 'C' shaped system, by three-dimensional trusses, composed by 4 ribbed rebars with diameter of 12 mm without overlapping, closed by small stirrups (Figure 1b). The yielding strength was equal to 518 and 451 N/mm^2 for rebars with diameter of 16 and 12 mm, respectively. Both reinforcement types had elastic modulus of about 194 kN/mm^2, and were placed at regular spacing of 780 mm. Horizontal

reinforcement was constituted by 2 ribbed rebars with diameter of 6 mm (yielding strength of 440 N/mm^2), distributed each other bed joint, (reinforcement percentage of about 0.04%). Mortar was developed on purpose to be used for bed joint laying and for filling vertical cavities. Its compressive strength was 11.3 N/mm^2 and the elastic modulus was 11.3 kN/mm^2.

2.2. Basic Characterization

The main issue of the testing program was to assess the behavior of the two reinforced masonry systems under out-of-plane cyclic actions. Tests were repeated on two series of specimens, named rmH and rmC respectively for specimens with 'H' and 'C' shaped units, and built adopting the construction systems described in previous section. Tests on reinforced masonry specimens were preceded by mechanical characterization of materials. Basic characterization of reinforced masonry walls was carried out by uniaxial compression and flexural tests. Three specimens for each test series and for each experiment type were tested. Finally, cyclic out-of-plane tests on two real scale structures, each constituted by two reinforced masonry walls, were carried out. The complete description of the test program and the results of the basic characterization are reported in Mosele et al. (2008).

In synthesis, behavior of the two construction systems was quite similar under uniaxial compression. Their average compressive strength was 4.62 N/mm^2 and the elastic modulus was 3.3 kN/mm^2. Flexural tests, which were preparatory for out-of-plane cyclic tests, were characterized by attainment of three main limit states: cracking, maximum resistance, and ultimate limit state, which was fixed when strength degradation of 20% occurred. Table 1 lists load and displacement values and their ratios for both reinforced masonry types. Flexural behavior until attainment of first limit state was similar for the two reinforced masonry systems, with opening of first flexural cracks on three central bed joints, at about 25% and 13% of maximum load. The higher percentage of vertical reinforcement of rmC system (almost twice that of rmH) affected the flexural behavior, provoking higher stiffness in cracked condition and different failure mechanism. Balanced failure, characterized by simultaneous yielding of rebars and crushing of units, was observed for rmC specimens; while for rmH specimens maximum resistance was attained only with rebars yielding. The higher strength reached with different failure mechanism influenced the displacement capacity of rmC walls, which at ultimate limit state was 24% smaller than for rmH specimens.

Table 1 Average results of flexural test

Test series	L_{cr} (kN)	d_{cr} (mm)	L_{max} (kN)	d_{Lmax} (mm)	L_u (kN)	d_u (mm)	$L_{cr/max}$ (-)	$d_{cr/Lmax}$ (-)	$d_{u/Lmax}$ (-)
RmH	17.5	1.9	69.2	17.4	55.3	74.7	0.25	0.11	4.29
RmC	16.9	1.3	132.2	23.4	105.5	56.9	0.13	0.06	2.43

3. OUT-OF-PLANE CYCLIC TESTS ON REAL SCALE STRUCTURES

3.1. Test set-up

Specimens for real scale out-of-plane cyclic tests were constituted by two reinforced masonry frames, each made of two walls, 6 m in height and 2 m in length, connected at the top by a heavy slab. The two pairs of walls were built one with 'H' shaped units and vertical reinforcement of one ribbed rebar with diameter 16 mm every 780 mm (percentage of reinforcement of 0.10%), the other one with 'C' shaped units and vertical reinforcement of four ribbed rebars with diameter 12 mm every 780 mm (percentage of reinforcement of 0.18%). Bottom reinforced concrete bond beams were fixed to the reaction slab, while the heavy slab was hinged at the top of the two walls. The slab was used to transfer horizontal displacements and simulate the effect of roof dead load. The walls were thus tested with cantilever boundary conditions, to reproduce the behavior described in the introduction. Figure 2 shows the test set-up. The steel reaction frame between the two reinforced masonry frames was used to apply lateral loads by means of hydraulic jack.

The roof dead load was calculated assuming single-story tall buildings with deformable roof and span from 10 to 15 m, typical for the building type taken into account. In the case of uniform load distribution, the roof dead load on walls changes, on the basis of span and roof type, from 10 to 30 kN/m. The heavy slab had mass of 10 t, which corresponded to about 25 kN/m. This load, close to the highest in the range of roof dead-loads, was chosen in order to emphasize instability effects due to out-of-plane deformations of walls (P-Δ effects).

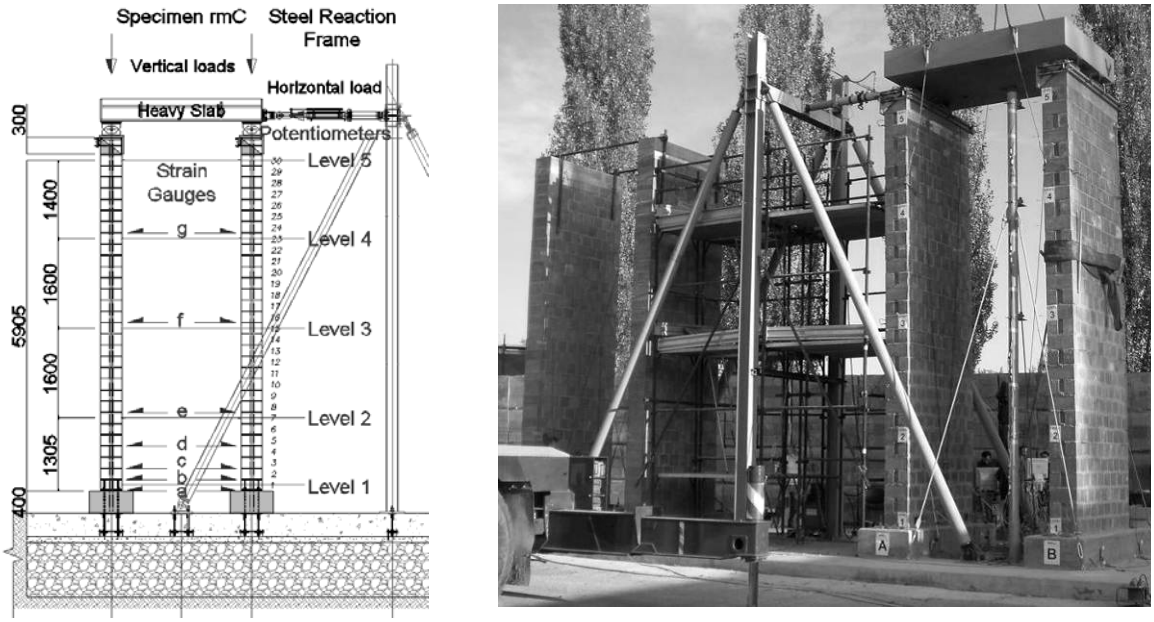

(a) (b)

Figure 2 Real scale out-of-plane cyclic test set-up

Lateral out-of-plane cyclic displacements with increasing amplitude were applied at constant frequency of 0.004 Hz and up to top displacement of ±250 mm. Displacement history was fixed by evaluating displacements at cracking and at maximum resistance in presence of second order effects, for the two specimens. The final part of the test, in the case of rmC walls, was carried out under monotonic loading, still under displacement control.

Each test specimen was instrumented with 64 sensors: 16 draw wire sensors (500 mm), placed at four heights along the walls, to measure the wall deflections (Level 2 to 4, Figure 2a); 4 potentiometers (±100 mm) at the walls' base (Level 1); other 12 potentiometers (±50 mm and ±25 mm) at the bottom bond beam. The remaining instruments were strain gauges (3 mm and 6 mm), placed on the vertical reinforcement at seven heights along the walls (from a to g, Figure 2 (a)).

3.2.Test Results

Figure 3 shows lateral loads applied at the top of the specimens versus displacements at the five monitored levels. Typical flexural behavior with presence of P-Δ effects was observed. Behavior in terms of strength, displacement capacity and influence of second order effects, was different for the two tested reinforced masonry systems.

Tests were characterized by attainment of three main limit states. The opening of first cracks at unit-bed joint interface occurred at top displacement d_{cr} of about 12.2 mm, for corresponding load levels L_{cr} of 8 and 10.25 kN for rmH and rmC, respectively (Table 2). Cracking continued within the first four courses up to 40 mm displacements. Within this interval, behavior of rmH specimen showed strong non-linearity, while cracking was quite uniform for rmC specimen, as can be seen by envelope curves shown in Figure 4c. Subsequently, cracks propagated on walls' height, and increased their width. They reached 13th bed joint on rmH specimen and 20th bed joint on rmC specimen. Maximum lateral load capacity L_{max} was attained for displacement levels, d_{Lmax}, at which the increase of bending

moment due to P-Δ effects was higher than the increase of resisting bending moment related to lateral displacements.
In the case of rmH specimen, L_{max} was reached almost at rebars' yielding (see Figure 5d), for top displacements of 165 mm, and with relevant bulging of wall at mid-height. Maximum attained displacement, d_{max}, was equal to 198 mm (see Figure 4b and c). Maximum lateral load capacity of rmC specimen, conversely, was reached under monotonic loading conditions, for top displacements d_{Lmax} of 310 mm, when crushing of units and yielding of rebars (Figure 5b) started. The following testing phase, up to maximum displacement d_{max} of 388 mm (Figure 4a and c), was thus characterized by exploitation of walls' full flexural strength, with bottom flexural cracks increasing their width and units crushing up to the third masonry course. Figure 4c shows how flexural stiffness in cracked phase was of basic importance for the out-of-plane behavior of tall walls. When rmH specimen reached L_{max}, displacement of rmC specimen, that had just entered the cracked phase, was six times smaller than for rmH. Figure 5 shows deflection profiles of walls (Figure 5a; c) and deformation of vertical reinforcement measured by strain-gauges at different heights (Figure 5b; d). These diagrams allow individuating a zone, at the wall base, along which vertical reinforcement deformation is constant. This can be related to the effects of second order moment, as Figure 6 shows. The measured deformation, for advanced test phases, indicates the formation of a plastic zone at the walls' base, which very likely extended for 1.2÷1.4 m of height for rmH walls (Figure 5d), and was limited to 1 m for rmC specimen (Figure 5b). In the case of rmC frame, crushing of units occurred on the first three courses of walls, and curvature was concentrated there (Figure 5a).

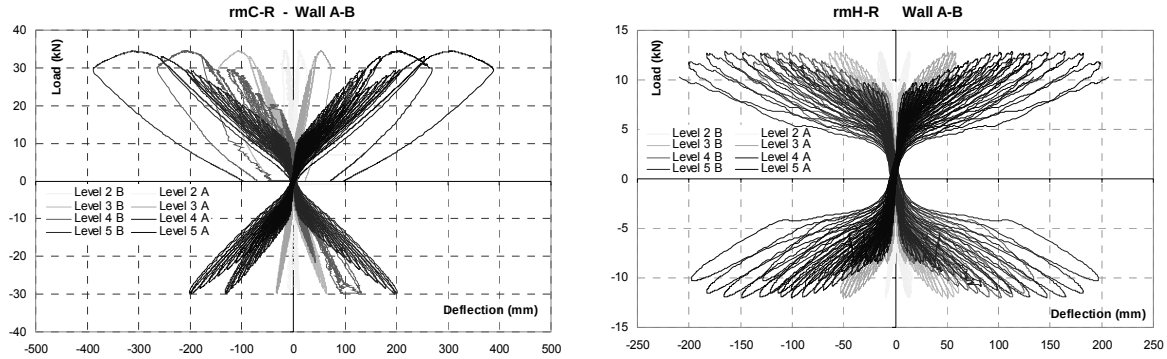

(a) rmC (b) rmH

Figure 3 Load-deflection cycles at the top monitored level

Table 2 gives load/displacement levels at main limit states, and some significant load and displacement ratios. Even if ratio between maximum displacement and displacement at maximum lateral load is similar for the two reinforced masonry systems, global displacement capacity of rmC specimen was twice than rmH. Ratio between load at first cracking and maximum load is equal to 64% for rmH specimen, and 30% for rmC. This means that cracked phase was limited for rmH specimen, and soon after opening of first cracks, increase of second order moment was higher than increase of sectional resistant moment. Conversely, rmC specimen presented an extended and stable cracked phase; i.e., this reinforced masonry system seems to be less affected by instability due to vertical loads.

Table 2 Cyclic out-of-plane test results

Specimen	L_{cr} (kN)	d_{cr} (mm)	L_{max} (kN)	d_{Lmax} (mm)	L_{dmax} (kN)	d_{max} (mm)	$L_{cr/max}$ (-)	$L_{dmax/max}$ (-)	$d_{cr/Lmax}$ (-)	$d_{max/Lmax}$ (-)
RmH	8.00	12.2	12.44	164.8	11.09	197.4	0.64	0.90	0.07	1.20
RmC	10.25	12.2	34.41	310.1	29.27	387.6	0.30	0.85	0.04	1.25

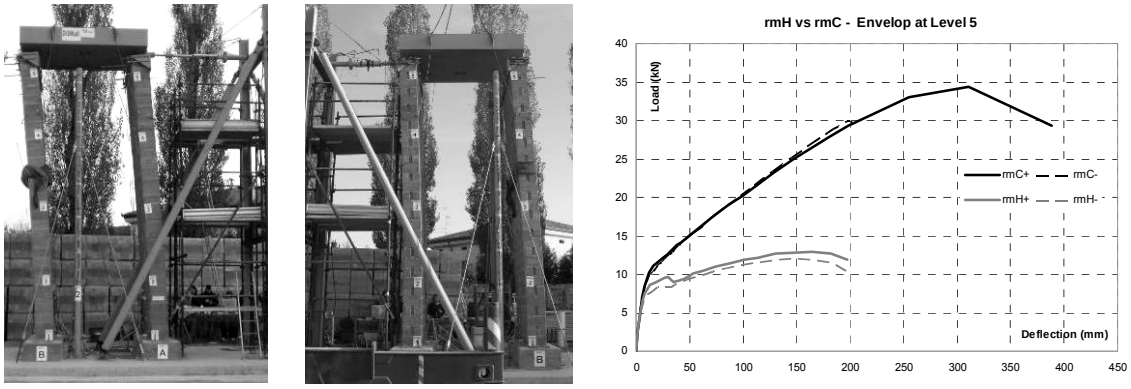

(a) rmC (b) rmH (c)

Figure 4 Deflection at the end of test (a and b); load-deflection envelope at the top level for the two reinforced masonry specimens

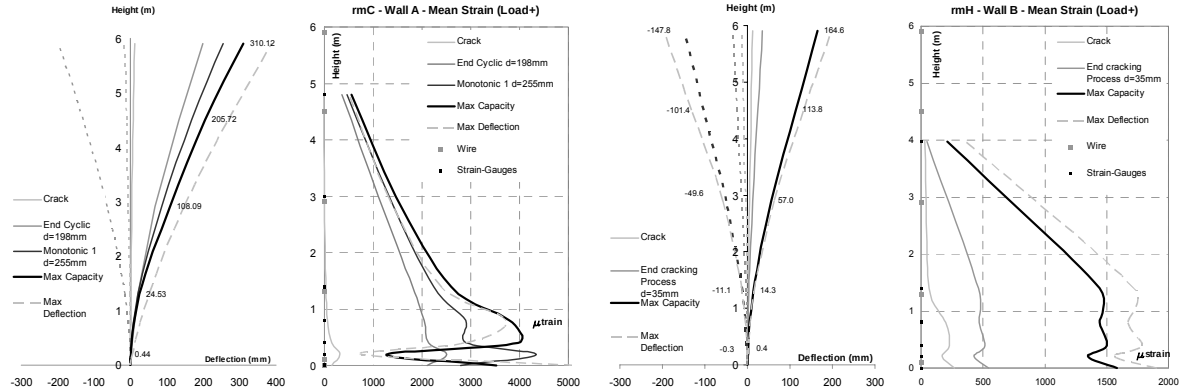

(a) rmC (b) rmC (c) rmH (d) rmH

Figure 5 Deflection profiles, average values (a and c); vertical reinforcement strain profiles (b and d)

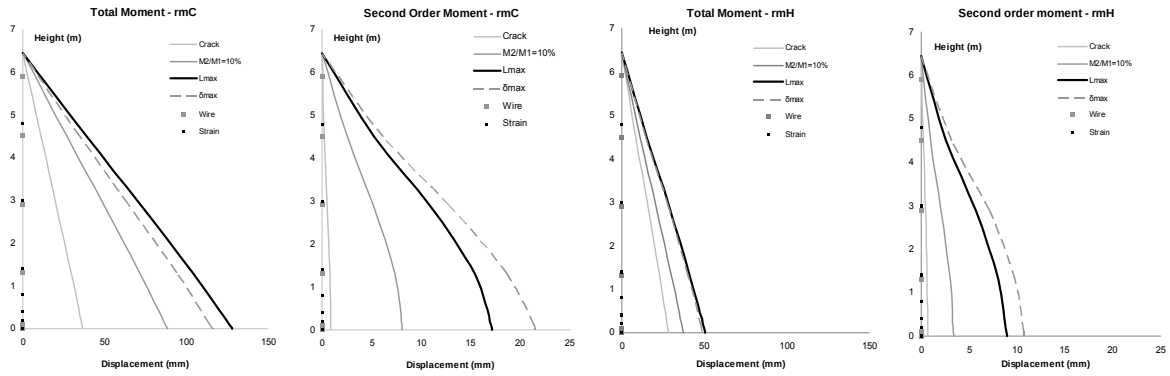

(a) rmC (a) rmC (c) rmH (d) rmH

Figure 6 Total bending moment on the walls' height (a and c); second order moment (b and d)

4. BENDING MOMENT ANALYSIS

Test results, in terms of bending moment, were analyzed to clarify influence of second order effects due to geometrical non-linearity. Measurement of applied horizontal loads allows obtaining first order bending moment; while measured displacements allow calculating second order moment due to vertical loads on walls' top, other than masonry self-weight. Figure 7 shows total (M), first order (M_1) and second order moment (M_2) at the base of each wall of the two specimens versus displacements

measured at the top.
Influence of second order effects is usually evaluated by stability ratio (Pettinga 2007), which is the ratio between second order moment and first order moment (M_2/M_1). According to Eurocode 2 for reinforced concrete structures, second order effects should be taken into account when stability ratio is higher than 10% (EN 1992-1-1, 2004). Table 3 lists stability ratio and bending moments at four states: the three limit states plus the state when stability ratio is 10%, which was thus assumed also in this case, to evaluate influence of second order effects on the two tested reinforced masonry systems.
At the beginning of test, vertical loads provided negligible contribution to bending moment in both reinforced masonry specimens (Figure 7); at crack limit state, in fact, stability ratio was very low (2.0÷2.5%, see Table 3). When displacements increased, stiffness of walls decreased and second order effects started to substantially influence flexural behavior of specimens. Stability ratio of 10% was reached by rmH walls for top displacement of 62.2 mm, and corresponding lateral load of 5.2 kN, which is 84% of maximum load capacity. RmC specimen reached the same stability ratio for displacement of 146.4 mm, and corresponding lateral load of 12.5 kN, which is 73% of maximum load capacity. At maximum load and maximum displacement limit states, influence of second order effects, in terms of stability ratio, was always smaller in rmC specimen (respectively 15.4 and 22.8% instead of 21.4 and 28%), despite higher displacement reached (310.1 and 387.6 mm instead of 164.8 and 197. 4). Bending moment analysis thus confirms experimental evidence, i.e. rmC system is able to withstand second order effects with higher safety level, and for higher displacements, than rmH, which in similar conditions is at its resistant capacity limit.

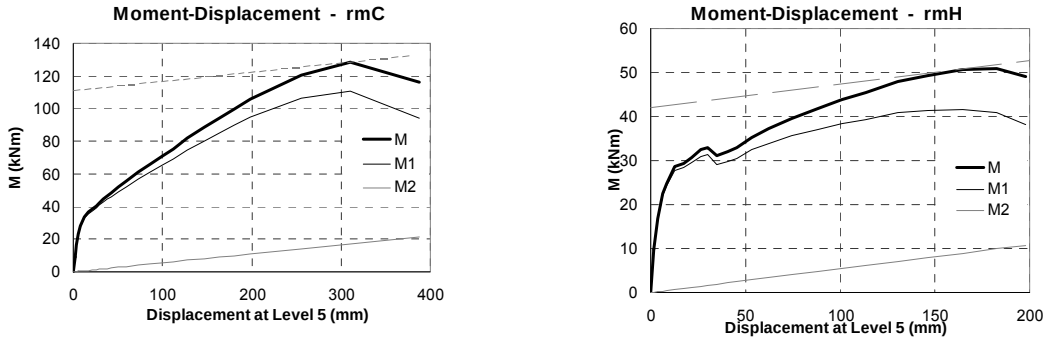

(a) rmC (b) rmH

Figure 7 Moment versus displacement curves for the two reinforced masonry systems

Table 3 Stability ratio at significant limit states

Limit State	Crack		10%		L_{max}		d_{max}	
	rmH	rmC	rmH	rmC	rmH	rmC	rmH	rmC
L/2 (kN)	4.0	5.1	5.2	12.5	6.2	17.2	5.5	14.6
d (mm)	12.2	12.2	62.2	146.4	164.8	310.1	197.4	387.6
M_1 (kNm)	27.83	33.07	33.81	80.32	41.66	110.96	38.28	94.41
M_2 (kNm)	0.69	0.68	3.38	8.05	8.93	17.13	10.71	21.53
M (kNm)	28.53	33.75	37.20	88.36	50.59	128.09	48.98	115.94
M_2/M_1 (%)	2.5	2.0	10.0	10.0	21.4	15.4	28.0	22.8

4. CONCLUSIONS

Slender load-bearing reinforced masonry walls, used for single-story tall buildings with deformable roofs such as commercial and industrial buildings, can be stressed by relevant out-of-plane loads, able to activate second order effects. Experimental tests were carried out in order to verify cyclic out-of-plane behavior with the influence of second order effects on two similar reinforced masonry systems, built with ‘H’ shaped and ‘C’ shaped perforated clay masonry units.

Out of plane cyclic tests confirmed the higher stiffness of rmC masonry type. Maximum horizontal load capacity was almost three times higher than for rmH system, but also maximum attained displacement was almost twice that of rmH system. Different behavior was also due to different impact of second order effects, which in the case of rmH system is higher than for rmC, as the earlier attainment of 10% stability ratio and the low increase of resistance from crack to maximum load limit state indicate. In the case of rmC system, the higher percentage of vertical reinforcement and its placement allow exploiting the masonry section strength and reducing the influence of second order effects.
Stability ratio shows that, for both systems, the top displacement which is necessary to activate the effective influence of second order effects is quite high: 62 mm and 146 mm respectively for rmH and rmC specimen. Those displacements correspond to about 1.0% and 2.5% of the walls' height. The fact that limit stability ratio for rmC specimen occurs for a ratio of lateral applied load to maximum load which is lower than for rmH, means that rmC system is able to resist second order effects with higher safety level, despite the higher displacements reached.

ACKNOWLEDGEMENTS

The present work was carried out under the framework of the European Contract COOP-CT-2005-018120: 'Developing Innovative Systems for Reinforced Masonry Walls - DISWall'. The enterprises involved in the production of the described system, Cis Edil s.r.l. and Tassullo S.p.A., were partners of the project.

REFERENCES

Bean Popehn, J.R., Schulz, A.E. and Drake, C.R. (2007). Behaviour of slender, post tensioned masonry walls under transverse loading. *ASCE Journal of Structural Engineering* **133:11,** 1541-1550.
European Committee for Standardization. (2004). EN 1992-1-1: Eurocode 2 - Design of concrete structures - Part 1-1: General rules and rules for buildings. Brussels.
Ewing, R.D. and Kariotis, J.C. (1981). Methodology for the mitigation of seismic hazards in existing unreinforced masonry buildings: wall testing, out of plane. ABK Topical Rep. no. 4, El Segundo, California.
Griffith, M.G., Lam, N.T.K., Wilson, J.L. and Doherty, K. (2004). Experimental investigation of unreinforced brick masonry walls in flexure. *ASCE Journal of Structural Engineering* **130:3,** 423-432.
Mosele, F., da Porto, F., Dalla Benetta, M. and Modena, C. (2008). Out-of-plane behaviour of tall reinforced masonry walls. Proc. 2nd Canadian Conference on Effective Design of Structures, McMaster University, Hamilton, Ontario, Canada, May 20–23, 2008; 289-300.
Pettinga, J.D. and Priestley, M.J.N. (2007). Accounting for P-Delta Effects in Structures when using Direct Displacement-Based Design, IUSS Press, Pavia.
Shing, P.B., Schuller, M. and Hoskered, V.S. (1990). Strength and ductility of reinforced masonry shear walls, *ASCE Journal of Structural Engineering* **116:3,** 619-640.
Simsir, C.C., Aschheim, M. A. and Abrams D.P. (2003). Influence of diaphragm flexibility on the out-of-plane response of unreinforced masonry bearing walls, Proc. 9th North American Masonry Conference, Clemson, South Carolina, 779-790
Tomaževič, M. (1999). Earthquake-resistant design of masonry buildings, Imperial College Press, London, UK.